Molecular Orientation Study of Methylene Blue at an Air/Fused-Silica Interface Using Evanescent-Wave Cavity Ring-Down Spectroscopy

ARTICLE *in* THE JOURNAL OF PHYSICAL CHEMISTRY B · APRIL 2005

Impact Factor: 3.3 · DOI: 10.1021/jp045290a · Source: PubMed

Molecular Orientation Study of Methylene Blue at an Air/Fused-Silica Interface Using Evanescent-Wave Cavity Ring-Down Spectroscopy

Fuping Li and Richard N. Zare*

Department of Chemistry, Stanford University, Stanford, California 94305

Received: October 14, 2004; In Final Form: December 7, 2004

Using evanescent-wave cavity ring-down spectroscopy (EW-CRDS), we monitored the change in the absorbance of a thin film of methylene blue (MB) at an air/fused-silica interface while varying the polarization of the incident light (600 nm). We derived the average orientation angle of the planar MB molecules with respect to the surface normal and observed that the average orientation angle decreases as the surface concentration increases. At low surface concentrations, the MB molecules lie almost flat on the surface, whereas at higher surface concentrations the molecules become vertically oriented.

Introduction

Organic thin films have unique chemical, optical, electronic, and mechanical properties that have been applied to such areas as light-emitting diodes,[1,2] solar cells,[3−5] and chemical sensors.[6,7] These molecular characteristics are affected by the way molecules assemble on the surface: that is, the interactions between the adsorbed molecules with each other and with the substrate. Thus, the characterization of the interfacial ordering of molecules, such as the average orientation angle, is of much interest.

Over the past twenty years, many spectroscopic techniques have been utilized to investigate the average molecular orientation at the interface, such as second-harmonic generation,[8−11] fluorescence,[12] attenuated total internal reflection,[12,13] linear dichroism,[12,14,15] and photoacoustic spectroscopy.[11]

Recently, cavity ring-down spectroscopy (CRDS) has also been used to carry out molecular orientation studies. Pipino[16] first implemented CRDS for this application in 2000 with the aid of a monolithic folded resonator to probe the molecular orientation of I_2 molecules adsorbed onto a curved surface. CRDS is a relatively new absorption technique for the measurement of weak optical transitions. This technique was first demonstrated in its present form by O'Keefe and Deacon[17] in 1988. A simple CRDS setup consists of a coherent light source, an optical resonator formed by two highly reflective mirrors facing each other, and a photodetector. When a pulse of light enters the cavity through the back of one mirror, it bounces back and forth inside the cavity, leaking out a small amount of light at each mirror. The photodetector records the decay of light intensity from behind the second mirror. The envelope of this decay is an exponential function, commonly referred to as the ring-down profile. The decay function for the light intensity is $I(t) = I_o e^{-t/\tau}$, where τ is the ring-down lifetime and depends on all losses of light within the optical cavity. The value of τ can be calculated from the expression $\tau = l/c(\Lambda_o + \Lambda_a)$, where l is the path length of the cavity, c is the speed of light in the cavity medium (assuming the refractive index is near unity), Λ_o is the light loss caused by the mirrors and other optics within the empty cavity, and Λ_a is the light loss induced by the absorber placed in the cavity. A comparison of ring-down lifetimes for an empty cavity and for one containing an absorber allows for the extraction of the absorbance of the analyte in a very simple manner.

The benefit of using CRDS over other absorption techniques is twofold. First, the intrinsically long path length increases the sensitivity of the technique. Second, the rate of the exponential decay does not depend on the initial light intensity, so that CRDS is relatively insensitive to fluctuations in laser pulse intensity. This technique has been used in gas-phase,[18,19] solid-phase,[20,21] and liquid-phase[22−24] studies. Pipino et al.[21] developed a variation of CRDS known as evanescent-wave cavity ring-down spectroscopy (EW-CRDS) to probe species at the air−solid interface. In this technique, a prism is placed in the optical cavity so that light undergoes total internal reflection at the prism surface, forming an evanescent wave. The electric field amplitude of the evanescent wave decays exponentially with distance from the surface. The penetration depth of the evanescent wave is on the order of a few hundred nanometers, depending on the wavelength of the incident light, the relative refractive index of the two media $n_{21} = n_2/n_1$, and the incident angle at the prism surface.

Evanescent-wave cavity ring-down spectroscopy is a very sensitive and surface-specific technique. Although EW-CRDS has been demonstrated using a variety of systems, to date there has been no systematic concentration-dependent molecular orientation study with this technique. For this purpose we chose to examine the concentration-dependent behavior of a planar molecule, methylene blue (MB), adsorbed to a fused-silica surface. Figure 1 shows the structure of the MB molecule and the UV−vis bulk absorption spectrum of 10 μM MB in methanol. As evident in the absorption profile, two major peaks appear, one near 600 nm and the other near 655 nm, both of which are attributed to the MB monomer under these conditions. It is known that MB dimerization or aggregation occurs not only in aqueous solution[25] but also on a surface.[26,27] Figure 2 shows the UV−vis absorption spectrum of a thin film of MB at a surface concentration of 1×10^{14} molecules/cm^2, which represents approximately full surface coverage. According to Ohline et al.,[26] H-type dimers (sandwich-type dimers) with an absorption peak around 600 nm is the dominant form of dimerization up to a surface concentration of 6.6×10^{14} molecules/cm^2. Beyond this concentration, J-type (bent) dimers appear, which weakly absorb around 690 nm. In our study, the surface concentration ranged from 1×10^{12} to 6×10^{14} molecules/cm^2 and the wavelength was set at 600 nm. Thus,

10.1021/jp045290a CCC: $30.25
Published on Web 02/03/2005

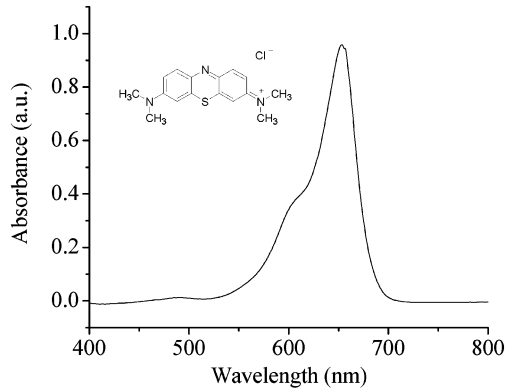

Figure 1. Structure of methylene blue and the UV−vis bulk absorption spectrum of 10 μM MB in methanol.

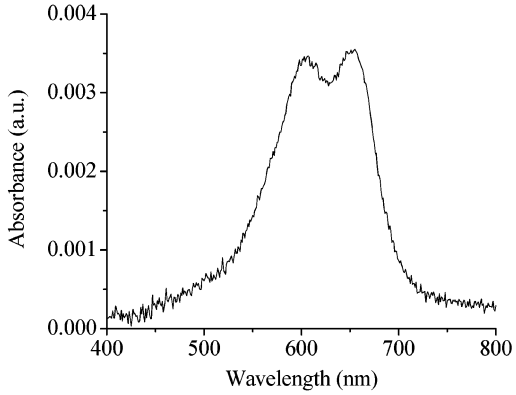

Figure 2. UV−vis absorption spectrum of MB at the surface concentration of 1×10^{14} molecules/cm^2.

the absorbance we measured is primarily that of MB monomer and H-type dimer.

The transition dipole moment of the MB molecule for both monomer and H-type dimer[28,29] lies along the main molecular axis; therefore, the absorbance depends on the polarization of the incident light with respect to the orientation of the molecular axis for both species. Our system is able to measure small absorbances on the order of 10^{-5} absorbance units, which enables us to measure the polarization-dependent variation in the absorbance at a small fraction of a monolayer. We measured the absorbance while the incident light was changed from *p*-polarization to *s*-polarization. By fitting the absorbance data with the aid of a theoretical model described below, we obtained the average orientation angle of the MB molecule (monomer and H-type dimer) with respect to the surface normal. We recorded polarization data for MB thin films whose thickness ranges from less than one-fiftieth of a monolayer to multilayers. We find that as the film thickness increases, the average orientation angle decreases.

Experimental Methods

EW-CRDS Apparatus. Figure 3 shows a schematic diagram of the experimental configuration employed in the EW-CRDS measurements. The pulsed (20 Hz) green light (532 nm) from a Nd:YAG laser (Spectra Physics) pumps a dye laser containing rhodamine 610, resulting in less than 2 mJ of 600 nm light with a pulse duration of 10 ns. The light passes through a vertically oriented linear polarizer to give *p*-polarized light. The polarization of the light incident on the optical cavity is controlled by a half-wave plate. The light leaking from the back of the second mirror is detected and amplified by a photomultiplier tube

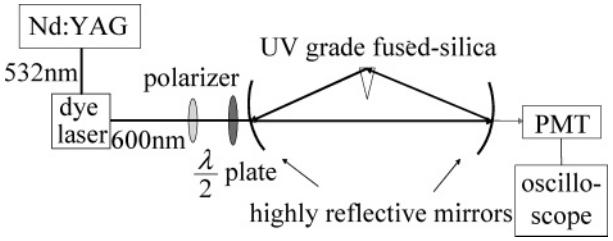

Figure 3. EW-CRDS experimental setup.

(R4632, Hamamatsu Corporation). The signals are then transferred to a LeCroy oscilloscope (LT342) and processed by a PC.

Instead of using a linear optical cavity, we constructed a ring cavity formed by two highly reflective mirrors (Newport, 1 m radius of curvature), each at a 20° angle, and a triangular fused-silica prism (Rocky Mountain Instrument); see Figure 3. The reflectivity of the mirrors is at least 99.97% over the broad wavelength range from 583 to 663 nm. The prism is specially designed in the shape of a 40° isosceles triangle. The two faces of the prism for which the light enters and exits have 600 nm antireflection coatings with $R < 0.00667\%$ for one side and $R < 0.01241\%$ for the other side. The top of the prism is polished to a flatness of $\lambda/20$ with a roughness of less than 0.4 nm rms. The evanescent wave is formed at this surface. The relative refractive index is $n_{21} = 1/1.46$ and the incident angle within the prism is 70°, resulting in an evanescent field penetration depth of approximately 148 nm.

This design reduces optical losses while allowing for the polarization to be changed. At the same time, the polarization of light inside the cavity is well maintained because possible polarization changes caused by the mirrors or the prism are not detectable under our experimental conditions. The ring cavity has a round-trip time of 3.54 ns and a ring-down lifetime of 1.6 μs or longer, corresponding to an intrinsic loss of $\Lambda_o = 0.0022$ or less. We average 20 individual ring-down lifetimes, resulting in a shot-to-shot variation in the ring-down lifetime (σ/τ) of 0.01. Thus, the minimum detectable absorption[30] is $(\Lambda_{abs})_{min} = \sqrt{2} \times \Lambda_o \times (\sigma/\tau) = 3 \times 10^{-5}$ absorbance units.

Molecular Orientation Measurements. The relative difference in the absorbance values obtained from *p*- and *s*-polarized light in an empty ring cavity was less than 1%. These absorbance values constitute the background. Solutions of MB were prepared in anhydrous methanol with concentrations ranging from 1 to 600 μM. For each data set, 10 μL of MB solution at a particular concentration was placed on the top surface of the prism. After the methanol had totally evaporated, a process that takes approximately 5 min, a self-assembled film of MB was formed with a surface area of 6 ± 0.3 cm^2. The absorbance of the methylene blue thin film was measured while changing the linear polarization of the light. Different MB solutions were examined with concentrations in the order from low to high. The prism surface and sides were carefully cleaned with spectroscopic-grade methanol and acetone before each experiment, and the background was remeasured for each experimental run.

Results and Discussion

The transition dipole moment of the MB molecule is along the main axis as shown in Figure 4. The experimental axes are also shown in Figure 4: the *x* and *y* axes are parallel to the prism surface, the *z* axis is perpendicular to the prism surface, and the *xz* plane is the plane of incidence. Because the surface of the prism is isotropic, a rotational symmetry in the distribution

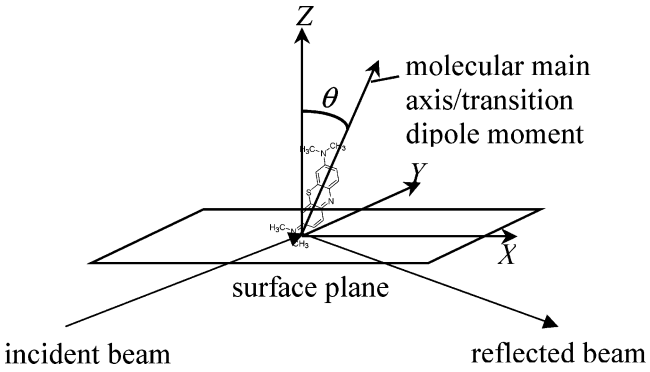

Figure 4. Schematic of a MB molecule adsorbed to the prism surface.

of the orientation angle with respect to the surface normal is assumed; that is, the *x* and *y* axes are equivalent.

The electric field of the evanescent wave at the prism surface has only one component in the *y* direction for *s*-polarized incident light, whereas it has two components for *p*-polarized incident light: one along the *z* direction and the other along the *x* direction. The difference in the responses resulting from this anisotropy is measured to determine the orientation of molecules on the prism surface.

The electric field amplitude of an evanescent wave at the surface in the rare medium is given by Harrick,[31] assuming a unit amplitude of incident light for both *s*- and *p*-polarization,

$$E_x = \frac{2(\sin^2 \alpha - n_{21}^2)^{1/2} \cos \alpha}{(1 - n_{21}^2)^{1/2}[(1 + n_{21}^2) \sin^2 \alpha - n_{21}^2]^{1/2}}$$

$$E_x = \frac{2 \cos \alpha}{(1 - n_{21}^2)^{1/2}}$$

$$E_z = \frac{2 \sin \alpha \cos \alpha}{(1 - n_{21}^2)^{1/2}[(1 + n_{21}^2)\sin^2 \alpha - n_{21}^2]^{1/2}} \quad (1)$$

where α is the incident angle and n_{21} is the relative refractive index of the two media. The absorbance measured in the experiment is

$$A = a|\langle g|\bar{p}\cdot\bar{E}|e\rangle|^2 \quad (2)$$

where *g* and *e* are the states involved in the dipole moment transition; *a* is the absorption coefficient; $\bar{p}$ is the transition dipole moment; and $\bar{E}$ is the electric field vector. This equation can be written

$$A = a\int_0^{\pi/2} \sin \theta \, d\theta \int_0^{2\pi} d\varphi \, f(\theta,\varphi)(pE_z \cos \theta + pE_{x,y} \sin \theta \cos \varphi)^2 \quad (3)$$

where θ is the orientation angle, $f(\theta,\varphi)$ is the orientation distribution function, and $E_{x,y}$ is the total electric field at the surface. Because the molecules are symmetric about the surface normal, $f(\theta,\varphi)$ can be written as $(1/2\pi)f(\theta)$. Therefore, the interfacial absorbance becomes

$$A = a\left(\langle \cos^2 \theta \rangle E_z^2 + \frac{1}{2}(1 - \langle \cos^2 \theta \rangle)E_{x,y}^2\right) \quad (4)$$

where $\langle \cos^2 \theta \rangle = \int_0^{\pi/2} \cos^2 \theta \, f(\theta) \sin \theta \, d\theta$. Here $\langle \cos^2 \theta \rangle$ represents the mean value of $\cos^2 \theta$ and is a measure of the mean orientation angle of the molecule. For *p*-polarized incident light, the absorbance A_p can be written as

$$A_p = a\left(\langle \cos^2 \theta \rangle E_z^2 + \frac{1}{2}(1 - \langle \cos^2 \theta \rangle)E_x^2\right) \quad (5)$$

and for *s*-polarized incident light, the absorbance A_s can be written as

$$A_s = a\left(\frac{1}{2}(1 - \langle \cos^2 \theta \rangle)E_y^2\right) \quad (6)$$

Thus, we obtain the expression

$$\langle \cos^2 \theta \rangle = \frac{E_y^2 A_p - E_x^2 A_s}{2E_z^2 A_s + E_y^2 A_p - E_x^2 A_s} \quad (7)$$

from which it follows that the average orientation angle of the MB molecule is given by

$$\langle \theta \rangle = \cos^{-1} \sqrt{\langle \cos^2 \theta \rangle} \quad (8)$$

Please note that $\langle \theta \rangle \neq \bar{\theta}$, where $\bar{\theta} = \int_0^{\pi/2} \theta \, f(\theta) \, d\theta$.

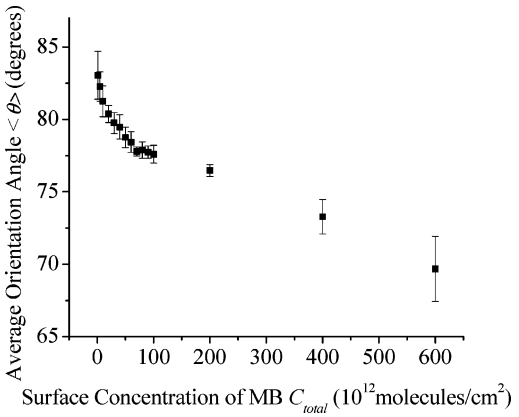

Figure 5. Trend of the average orientation angle $\langle \theta \rangle$ of MB molecules as a function of surface concentration C_{total}.

Figure 5 presents the average orientation angle $\langle \theta \rangle$ of the absorber, which is primarily monomer and a small contribution from H-type dimer MB molecules, versus the surface concentration C_{total}. We interpret our data to apply only to the MB monomer, as we cannot measure separately the contribution from the H-type dimer. The value of C_{total} is calculated from the product of the solution concentration and the volume (10 μL) divided by the film area ($\sim$6 cm^2). The average orientation angle decreases monotonically as the surface concentration of MB increases. At the lowest surface concentration in our experiment, which corresponds to a thickness of one-fiftieth of a monolayer, the average orientation angle is as high as 83° with respect to the surface normal. We conclude that the MB molecules lie almost flat on the fused-silica/air interface in the low-coverage limit. As the surface concentration increases, however, the average orientation angle gradually decreases. This trend implies that the MB molecules stand up and become more compact as the surface concentration increases instead of piling up on each other while maintaining the same orientation angle.

When the distribution of orientation angles is very large, $\langle \cos^2 \theta \rangle$ approaches the value of 1/3, corresponding to an average orientation angle of 54.7°, also known as the magic angle.[32] Under these circumstances, we cannot distinguish between a distribution in which the molecules are all nearly oriented at the magic angle and a distribution in which the orientation angles

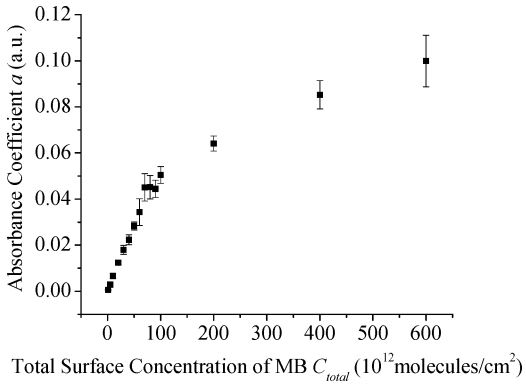

Figure 6. Absorption coefficient a versus the total surface concentration C_{total}.

are uniformly distributed. In our experiment, the smallest average orientation angle is about 70°, far away from the magic angle. This behavior suggests that the distribution of the orientation angles in our experiment is quite narrow for concentrations ranging up to full surface coverage.

Figure 6 shows how the absorption coefficient, a, varies with the total surface concentration C_{total}. According to Ohline et al.,[26] the surface concentration in our study is low enough that there is almost no higher order aggregation beyond that of the dimer. Thus, we need only consider the following equilibrium:

$$2M \overset{k}{\rightleftarrows} D; \qquad K = \frac{[D]}{[M]^2} \tag{9}$$

where M stands for monomer, D stands for dimer, and K is the equilibrium constant.

Conservation of mass allows us to write the relationship between the total surface concentration C_{total} and the monomer and dimer concentrations as

$$C_{\text{total}} = [M] + 2[D] \tag{10}$$

At relatively low surface concentrations, monomer is the primary species on the surface. The absorption coefficient, a, increases linearly with surface concentration up to the total surface concentration of 1×10^{14} molecules/cm^2. When the total surface concentration is above 1×10^{14} molecules/cm^2, the slope of absorption coefficient versus total surface concentration decreases. This behavior may indicate that the concentration of H-type dimers becomes appreciable. The smaller slope is consistent with the fact that the extinction coefficient of the dimer is about 6 times smaller than that of the monomer at 600 nm.[26,29]

In our experiment, we used an evaporation method to coat the prism surface and form the MB film. We also tried the drop-and-drag coating method and obtained similar results. Because of the prism geometry, other coating methods such as dip-coating and spin-coating cannot easily be applied to our system. We believe that the average orientation angle for methylene blue at the air/fused-silica interface is not affected by the coating method employed.

The present results are not surprising; instances have been reported in the literature where the average orientation changes with surface coverage.[9,14] What is presented here is a new technique for obtaining sensitive measurements of the orientation of molecules at an interface.

Acknowledgment. The authors would like to thank Dr. Kate L. Bechtel for valuable discussions. This material is based upon work supported by the National Science Foundation under Grant No. MPS-0313996.

References and Notes

(1) Dimitrakopoulos, C. D.; Malenfant, P. R. L. *Adv. Mater.* **2002**, *14*, 99.
(2) Sheridan, A. K.; Buckley, A. R.; Fox, A. M.; Bacher, A.; Bradley, D. D. C.; Samuel, I. D. W. *J. Appl. Phys.* **2002**, *92*, 6367.
(3) AlMohamad, A.; Soukieh, M. *Thin Solid Films* **1995**, *271*, 132.
(4) Peumans, P.; Yakimov, A.; Forrest, S. R. *J. Appl. Phys.* **2003**, *93*, 3693.
(5) Mccaffrey, R. R.; Prasad, P. N. *Solar Cells* **1984**, *11*, 401.
(6) Torsi, L.; Dodabalapur, A.; Sabbatini, L.; Zambonin, P. G. *Sens. Actuators B* **2000**, *67*, 312.
(7) Mukhopadhyay, S.; Hogarth, C. A.; Thorpe, S. C.; Cook, M. J. *J. Mater. Sci.: Mater. Electron.* **1994**, *5*, 321.
(8) Higgins, D. A.; Byerly, S. K.; Abrams, M. B.; Corn, R. M. *J. Phys. Chem.* **1991**, *95*, 6984.
(9) Kikteva, T.; Star, D.; Leach, G. W. *J. Phys. Chem.* **2000**, *104*, 2860.
(10) Florsheimer, M.; Bootsmann, M. T.; Fuchs, H. *Phys. Rev. B* **2002**, *65*, 125406/1.
(11) Simpson, G. J.; Westerbuhr, S. G.; Rowlen, K. L. *Anal. Chem.* **2000**, *72*, 887.
(12) Edmiston, P. L.; Lee, J. E.; Wood, L. L.; Saavedra, S. S. *J. Phys. Chem.* **1996**, *100*, 775.
(13) Picard, F.; Buffeteau, T.; Desbat, B.; Auger, M.; Pezolet, M. *Biophys. J.* **1999**, *76*, 539.
(14) Cropek, D. M.; Bohn, P. W. *J. Phys. Chem.* **1990**, *94*, 6452.
(15) Jang, W. H.; Miller, J. D. *J. Phys. Chem.* **1995**, *99*, 10272.
(16) Pipino, A. C. R. *Appl. Opt.* **2000**, *39*, 1449.
(17) Okeefe, A.; Deacon, D. A. G. *Rev. Sci. Instrum.* **1988**, *59*, 2544.
(18) Xie, J.; Paldus, B. A.; Wahl, E. H.; Martin, J.; Owano, T. G.; Kruger, C. H.; Harris, J. S.; Zare, R. N. *Chem. Phys. Lett.* **1998**, *284*, 387.
(19) Spence, T. G.; Harb, C. C.; Paldus, B. A.; Zare, R. N.; Willke, B.; Byer, R. L. *Rev. Sci. Instrum.* **2000**, *71*, 347.
(20) Pipino, A. C. R.; Hudgens, J. W.; Huie, R. E. *Chem. Phys. Lett.* **1997**, *280*, 104.
(21) Pipino, A. C. R.; Hudgens, J. W.; Huie, R. E. *Rev. Sci. Instrum.* **1997**, *68*, 2978.
(22) Hallock, A. J.; Berman, E. S. F.; Zare, R. N. *Appl. Spectrosc.* **2003**, *57*, 571.
(23) Snyder, K. L.; Zare, R. N. *Anal. Chem.* **2003**, *75*, 3086.
(24) Shaw, A. M.; Hannon, T. E.; Li, F.; Zare, R. N. *J. Phys. Chem.* **2003**, *107*, 7070.
(25) Giles, C. H.; Duff, D. G. *Water: A Comprehensive Treatise;* Franks, Ed.; New York, 1973.
(26) Ohline, S. M.; Lee, S.; Williams, S.; Chang, C. *Chem. Phys. Lett.* **2001**, *346*, 9.
(27) Kobayashi, H.; Takahashi, M.; Kotani, M. *Chem. Phys. Lett.* **2001**, *349*, 376.
(28) Antonov, L.; Gergov, G.; Petrov, V.; Kubista, M.; Nygren, J. *Talanta* **1999**, *49*, 99.
(29) Patil, K.; Pawar, R.; Talap, P. *Phys. Chem. Chem. Phys.* **2000**, *2*, 4313.
(30) Romanini, D.; Lehmann, K. *J. Chem. Phys.* **1993**, *99*, 6287.
(31) Harrick, N. J. *Internal Reflection Spectroscopy*; Wiley & Sons: New York, 1967.
(32) Simpson, G. J.; Rowlen, K. L. *Acc. Chem. Res.* **2000**, *33*, 781.